

Article

Developing Electrolyte for a Soluble Lead Redox Flow Battery by Reprocessing Spent Lead Acid Battery Electrodes

Keletso Orapeleng *, Richard G. A. Wills and Andrew Cruden

Energy Technology Group, University of Southampton, Southampton SO17 1BJ, UK; rgaw@soton.ac.uk (R.G.A.W.); a.j.cruden@soton.ac.uk (A.C.)

* Correspondence: ko1d13@soton.ac.uk; Tel.: +44-(0)23-8059-6727

Academic Editor: Joeri Van Mierlo

Received: 8 March 2017; Accepted: 27 April 2017; Published: 3 May 2017

Abstract: The archival value of this paper is the investigation of novel methods to recover lead (II) ions from spent lead acid battery electrodes to be used directly as electrolyte for a soluble lead flow battery. The methods involved heating electrodes of spent lead acid batteries in methanesulfonic acid and hydrogen peroxide to dissolve solid lead and lead dioxide out of the electrode material. The processes yielded lead methanesulfonate, which is an electrolyte for the soluble lead acid battery. The lead (II) ions in the electrolyte were identified using Inductively Coupled Plasma Mass Spectroscopy and their electrochemistry confirmed using cyclic voltammetry. The concentration of lead (II) ions was determined and it was found that using the higher concentration of hydrogen peroxide yielded the highest concentration of lead (II) ions. The method was therefore found to be sufficient to make electrolyte for a soluble lead cell.

Keywords: lead recovery; electrolyte; soluble lead flow battery; energy storage

1. Introduction

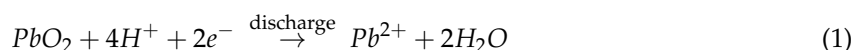
Energy storage is essential to enable uptake of renewable energy [1]. Lead acid batteries, a well-established technology that is accessible world-wide, emerged as a convenient technology for renewable energy storage applications in [2]. Despite being a mature technology and relatively low priced (£150/kWh), lead acid batteries are sensitive to incorrect use. They are sensitive to temperatures above the design 25 °C; releasing more energy at high temperatures but also deteriorating more quickly, which reduces battery life by as much as 50% for each 8–10 K temperature increase [2,3]. Discharging beyond 25% depth of discharge for starting, lighting and ignition (SLI) batteries results in accelerated deterioration [4]. Lead acid batteries need to be stored fully charged to avoid sulfation, and storage temperatures should not exceed 25 °C to slow down self-discharge [3]. When used with isolated PV systems, it is not always possible to charge the battery before storage as availability of electricity is dependent on local weather [2]. Even when used as recommended, the longest lasting lead acid (valve regulated) batteries last a maximum of five years, well before other components of a power generation system need replacing [2–5]. Redox flow batteries are emerging as a viable option for stationary energy storage [6–8]. This type of battery, depending on the technology, offers a complement of qualities superior to those of the conventional lead acid battery, including higher cycle-life, tolerance to deep cycling [8], tolerance to wider temperature ranges, better temperature control and faster charge and discharge rates [6]. Table 1 compares these qualities for selected redox flow batteries and the lead acid battery.

Table 1. Comparison of the lead acid battery to commercial flow batteries on energy density, cell voltage, cycle life and depth of discharge, energy efficiency and estimated cost.

Technology	Lead Acid	Soluble Lead Flow Battery	All Vanadium/ Vanadium–Bromine	Zinc–Bromine
Cell voltage, V	2.0 [5]	1.78	1.4/1.0 [1]	1.8
Energy efficiency, %	75–85 [9]	65% [10]	(80–85)/(60–70) [11]	65–75
Cycle life	200–2000	2000 [12]	12,000 [13]	10,000
@ Depth of Discharge	70%–30%	100%	100%	100%
Recommended operating temperature range, °C	20–25	35–55	(5–40)/(0–50) [11]	20–50
Cost, €/kWh	50–150 [14]	-	140–400 [15]	800

Unlike the vanadium and the zinc bromine redox flow batteries, the soluble lead flow battery (SLFB) uses comparatively cheap and non-corrosive materials in redox flow technology. The SLFB is a well-researched technology [10,16–18] that uses electrolyte made from methanesulfonic acid (MSA) and Pb^{2+} in the form of lead methanesulfonate. The electrochemistry is based on two redox couples; Pb/Pb^{2+} and PbO_2/Pb^{2+} [10]. The reactions are shown below in Equations (1)–(3) [16,19].

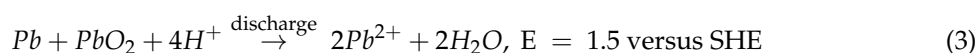
Positive electrode:



Negative electrode:



Overall:



where, SHE is standard hydrogen electrode.

During charge, lead metal is deposited on the negative electrode while lead (IV) oxide is deposited on the positive electrode. During discharge, the deposit from both electrodes is stripped back into the electrolyte as Pb^{2+} ions. Lower concentrations of lead ions in the electrolyte were found to be ideal for uniform and adherent deposit on both electrodes [20]. On the other hand, for higher cell charge capacities, higher concentrations are required. A concentration of $1.0 \text{ mol} \cdot \text{dm}^{-3} Pb^{2+}$ was sought as a compromise.

Since lead acid batteries, including automobile batteries, are globally available, there is an opportunity to use the lead contained therein in soluble lead flow batteries. Traditionally, lead acid batteries are recycled to recover lead and re-use it in making new batteries [21,22]. The most common method is the pyrometallurgic, which is energy intensive with operation temperatures above $300 \text{ }^\circ\text{C}$ and produces slag and air contaminants such as sulfur oxide, nitrous oxide and fumes [22]. This paper presents a method to make electrolyte for a soluble lead flow battery by harvesting lead directly from end-of-life lead acid batteries.

2. Experimental

2.1. Chemical Reagents

The chemicals used to make the electrolyte were methanesulfonic acid, lead methanesulfonate, and hydrogen peroxide. Aqueous solutions of the chemicals were prepared using de-ionised water from a Purite water purifier. Ethylenediaminetetrascetic acid (EDTA) was used in titration, as well as Eriochrome Black T indicator, ammonium hydroxide, ammonium chloride, tartaric acid, and sodium chloride. The chemicals are listed in Table 2, along with their purities as well as the chemical suppliers. Chemicals were used as received.

Table 2. Chemical reagents used in lead recovery as well as those used in titration. The chemical name and purity is given where appropriate, as well as the supplier's name.

Chemical	Molecular Formula	Purity/Concentration	Supplier
Methanesulfonic acid (MSA)	CH ₃ SO ₃ H	99%	Sigma Aldrich, London, UK
Lead methanesulfonate	Pb(CH ₃ SO ₃) ₂	50% w/w	Sigma Aldrich
Hydrogen peroxide	H ₂ O ₂	30% w/w	Sigma Aldrich
EDTA	C ₁₀ H ₁₆ N ₂ O ₈	99.4–100.6	Sigma Aldrich
Eriochrome Black T	C ₂₀ H ₁₂ N ₃ NaO ₇ S	-	Sigma Aldrich
Ammonium hydroxide	NH ₄ OH	28.0–30% NH ₃	Sigma Aldrich
Ammonium chloride	NH ₄ Cl	99.5%	Sigma Aldrich
Potassium chloride	KCl	99.5%	Fisher Scientific, Loughborough, UK
Tartaric acid	C ₄ H ₆ O ₆	99.5%	Sigma Aldrich

2.2. Sample

End-of-life Yuasa NP7-12L, 7 Ah 12 V Valve Regulated Lead Acid (VRLA) batteries were disassembled to extract lead from the battery electrodes. Each battery comprised six cells of ~2 V each as shown in Figure 1, each of which had five negative and four positive electrodes separated by an Absorbed Glass Mat (AGM). The electrodes were made of a mixture of carbon and lead oxide, and the grids a lead calcium alloy. The separator was soaked in 33.3% dilute sulfuric acid. Physical dimensions of the battery were 151 mm × 65 mm × 94 mm and a mass of 2.8 kg [23].



Figure 1. A 12 V lead acid battery with its lid sawn off to show the six compartments containing five negative and four positive electrode sets each. Lead current collectors are connected to each electrode and the positive connections connected together, as are the negative electrodes. The connection is maintained along the six cell in series, and terminate at two external leads.

2.3. Equipment

An LD300 DC electronic load (Huntington, UK) was used to discharge the sample batteries; Solartron equipment 1470E CellTest (West Sussex, UK) was used to measure the battery on open circuit, and to charge and discharge the batteries. For heating purposes, a water bath and Yellow Line MST basic C stirrer (Boutersem, Belgium) with a coated chemical-resistant heating base were used, and a TC 3 electronic contact thermometer was used to monitor the mixture temperature. A Sigma 2-6E centrifuge machine (Osterode am Harz, Germany) was used for liquid/solids separation. For mass measurements, a balance with precision $g \pm 0.001$ was used. Elemental analysis was performed using the Element 2XR Inductively Coupled Plasma Mass Spectrometer (ICP-MS, Thermo Fisher Scientific, Waltham, MA USA). Cyclic voltammetry was performed on an Autolab potentiostat (Metrohm, Utrecht, The Netherlands).

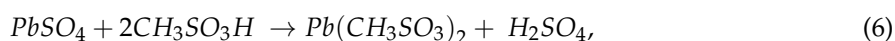
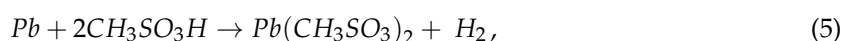
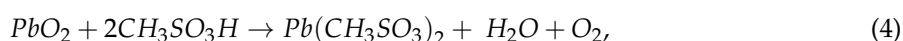
2.4. Development of Lead Recovery Method

Low energy chemical and mechanical methods were favoured for lead recovery. The following subsections explain the choice of treatment methods.

2.4.1. Use of Methanesulfonic Acid

The ability to dissolve the redox couple at both charged and discharged states is an important feature of an electrolyte [24]. Lead methanesulfonate solubility in water is high, at $2.6 \text{ mol}\cdot\text{dm}^{-3}$, compared to lead sulfate which saturates at $0.004 \text{ mol}\cdot\text{dm}^{-3}$, lead hydroxide at $0.034 \text{ mol}\cdot\text{dm}^{-3}$, or lead nitrate at $1.64 \text{ mol}\cdot\text{dm}^{-3}$ [25]. MSA retains good conductivity ($275 \text{ S}\cdot\text{cm}^{-2}\cdot\text{mol}^{-1}$), and has lower toxicity than other solvents. Where nitric acid reacts with metals to evolve hydrogen, MSA does not. MSA does not attack organic compounds nor does it require pre-disposal treatment like H_2SO_4 [25]. Therefore, MSA was used to make lead (II) methanesulfonate electrolyte.

The lead found in lead acid battery electrodes occurs as PbO_2 , PbSO_4 and Pb metal. MSA reacts chemically with these forms in the following ways:



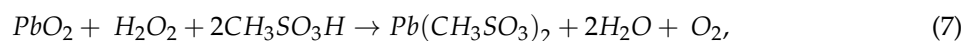
Empirically, the solubility limit of Pb in MSA is indicated at $1.25 \text{ mol}\cdot\text{dm}^{-3} \text{ Pb}^{2+}$ in $2.5 \text{ mol}\cdot\text{dm}^{-3}$ MSA at 25°C [19,25], while the solubility of lead methanesulfonate is inversely proportional to the concentration of methanesulfonic acid [19]. Reference [16] also shows that conductivity of electrolyte made from methanesulfonic acid increases with high acid concentrations and low lead concentration. On the other hand, more lead is required to yield more energy from the cell. The electrolyte acidity also reduces during discharge, as the concentration of Pb^{2+} ions in the electrolyte increases. It is therefore important to balance the concentrations to avoid precipitation of lead methanesulfonate salt into the cell when it is fully discharged. Pletcher et al. [26] recommend that the acidity of electrolyte made from Pb^{2+} and MSA should be limited to $2.4 \text{ mol}\cdot\text{dm}^{-3}$ MSA to prevent formation of flaky deposits in an electrochemical cell. Therefore, the concentration of MSA in this experiment was limited to $2.5 \text{ mol}\cdot\text{dm}^{-3}$, which would yield $1.0 \text{ mol}\cdot\text{dm}^{-3} \text{ Pb}^{2+}$ ions.

2.4.2. Heating

Lead (IV) oxide reacts with warm acids to form more stable lead (II) ions and release oxygen [27]. Heat was used to speed up the reaction between MSA and PbO_2 . As a preliminary measure, the heating temperature was limited to 50°C to minimise energy use.

2.4.3. Use of Hydrogen Peroxide

Hydrogen peroxide (H_2O_2) is capable of acting as a reducing agent as well as an oxidising agent in acidic conditions [28] (p. 600). It was used to reduce Pb (IV) oxide to Pb (II) ions in MSA, shown in Equation (7). It was also used to catalyse the oxidation of Pb metal to Pb (II) ions in MSA in Equation (8). These reactions occur faster than the oxide and metal reactions with acid. H_2O_2 has also been used to recondition a soluble lead cell to remove PbO_2 sludge build-up [18].



2.5. Lead Recovery Method

This section presents the procedure used to disassemble a 7 Ah 12 V VRLA battery and dissolve lead out of the battery electrodes.

2.5.1. Determining Battery State of Health

Before disassembly, the state of health (SoH) of the battery was determined. A 12 V SLI VRLA battery that maintains only 80% of its rated capacity in Ah is at the end of its service life [29]. According to the VRLA battery manual, a voltage of 12.6 V corresponds to 100% state of charge (SoC) while an open circuit voltage under 11.8 V indicates 0% SoC [30]. Therefore, the battery was galvanometrically cycled ten times between 12.6 V (100%) and 11.86 V (0% SoC), charging at 0.7 A (C/10) constant current for 3 h and discharging at the same rate for 3 h to determine how much Ah capacity it could retain. Its open circuit voltage was measured after charge.

2.5.2. Disassembling the Battery

The sealed battery was disassembled using the procedure below:

- (1) Sulfuric acid was emptied from the battery.
- (2) The battery was rinsed with distilled water three times.
- (3) The top cover of the battery was sawn off, and electrodes were retrieved out of each cell chamber as shown in Figure 2a,b.

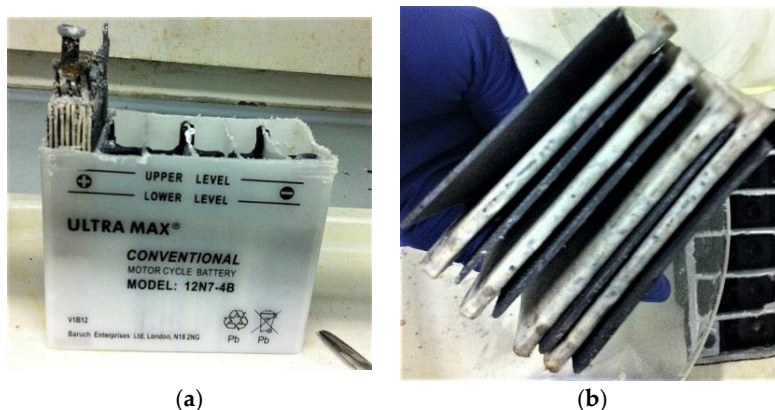


Figure 2. (a) A 12 V VRLA battery showing extraction of one of the six cells' contents; and (b) The multi-electrode assembly with Absorbed Glass Matt separator.

2.5.3. Dissolving Lead from Battery Electrodes

Each of the electrode sets retrieved from a battery was weighed and placed in a separate container to be investigated uniquely. In the first container, 500 mL of $2.5 \text{ mol}\cdot\text{dm}^{-3}$ MSA was added to the contents and heated to $30 \text{ }^\circ\text{C}$. Change in density of the solution formed was monitored and heating was maintained until the density of the solution plateaued. The procedure to monitor density is explained in Section 2.6 on measurement.

Electrodes in the second container were treated similarly except the acid was heated to $40 \text{ }^\circ\text{C}$. For the third experiment, 450 mL of $2.5 \text{ mol}\cdot\text{dm}^{-3}$ MSA was used and 50 mL of $0.09 \text{ mol}\cdot\text{dm}^{-3}$ hydrogen peroxide was added. The contents were heated to $30 \text{ }^\circ\text{C}$. In the fourth container, the temperature was increased to $40 \text{ }^\circ\text{C}$. In the fifth and sixth experiments, the hydrogen peroxide was diluted at $0.90 \text{ mol}\cdot\text{dm}^{-3}$ and the mixtures were heated to $30 \text{ }^\circ\text{C}$ and $40 \text{ }^\circ\text{C}$, respectively. The procedure is outlined in Figure 3.

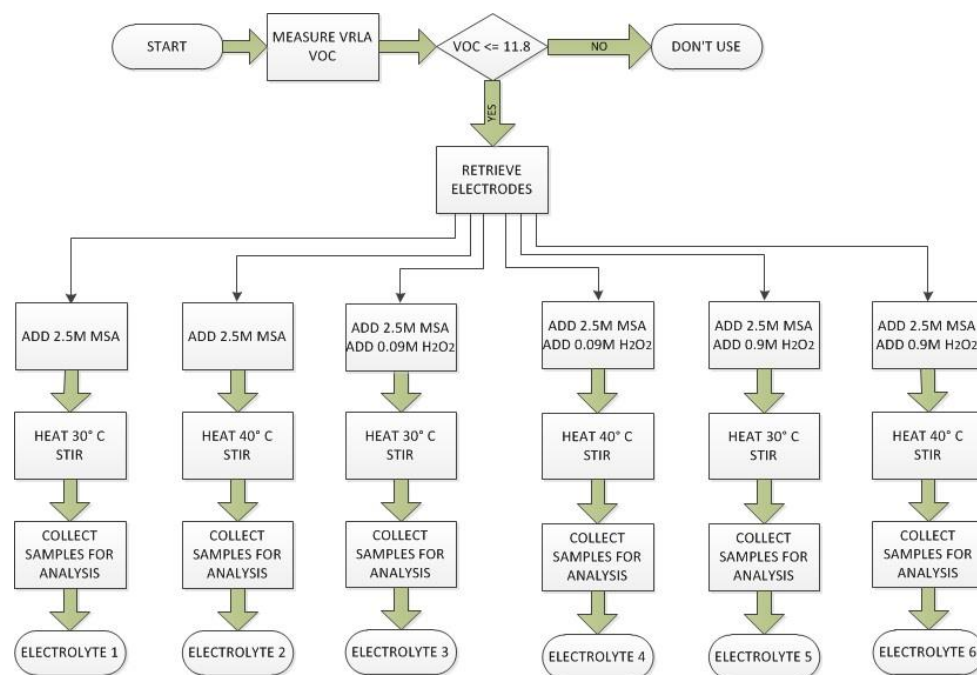


Figure 3. Lead recovery plan for electrolyte preparation. The electrodes retrieved from a spent VRLA battery with open circuit voltage less than 11.8 V were each placed in a beaker. An amount of $2.5 \text{ mol}\cdot\text{dm}^{-3}$ MSA was added to the electrodes. The contents were heated at either 30°C or 40°C . In the first two cases, no H_2O_2 was added, in the next two cases $0.09 \text{ mol}\cdot\text{dm}^{-3}$ H_2O_2 was added to the beaker while the last two had $0.90 \text{ mol}\cdot\text{dm}^{-3}$ H_2O_2 .

2.5.4. Electrolyte Preparation

The liquid from dissolving lead battery electrodes was separated from undissolved solids by centrifuging at 3600 rpm for 20 min. The supernatant liquid was collected and named “recovered electrolyte” and used as electrolyte in soluble lead cells. The metal composition of the electrolyte was determined using Inductively Coupled Plasma Mass Spectroscopy (ICP-MS.) The concentration of the Pb^{2+} ions was determined using mass measurements as well as titration as outlined in Sections 2.6.2 and 2.6.3, respectively.

2.6. Measurements

2.6.1. Inductively Coupled Plasma Mass Spectroscopy

ICP-MS allows analysis of trace elements which may otherwise be difficult to do using other analytical methods. The sample is pulverised into plasma using high currents, and the mist created is scanned for trace elements. Detection levels at parts per billion (ppb) can be realised.

Since the quantity of trace metals other than lead in the recovered electrolyte was expected to be low, ICP-MS was used. The manual for the VRLA battery mentioned that the grid of the battery was made of lead-calcium alloy [30]. Literature on lead acid batteries also mentioned that grids may also contain antimony and tin as alloying agents, as well as traces of bismuth [31–33]. The ICP-MS was therefore performed to check the presence of these elements as well as to quantify them.

2.6.2. Change in Mass of Solution

From each mixture, a sample was collected every hour and centrifuged at 3600 rpm for 20 min to separate the liquid from the solids. A 10 mL sample of the supernatant liquid was collected and its mass was measured and recorded. This was used to monitor the change in density of the solution. Assuming that the increase in mass of the clear solution was due to Pb and PbO_2 solids being converted

to Pb^{2+} ions, the concentration of Pb^{2+} ions was estimated from the change in mass, using Equation (9) below:

$$[Pb^{2+}] = \frac{\Delta m}{V_s MM_{Pb}} \quad (9)$$

where, $[Pb^{2+}]$ is the concentration of Pb^{2+} ions, in $\text{mol}\cdot\text{dm}^{-3}$; Δm is the change in mass of recovered solution over specific period, in grams; V_s is the volume of the sample weighed, in dm^3 ; MM_{Pb} is the molar mass of lead, in $\text{g}\cdot\text{mol}^{-1}$.

2.6.3. Titration

Complexometric titration of the sample with EDTA acid and Eriochrome Black T dye, as described by Fitch [34], was carried out to determine the concentration of Pb^{2+} ions in the solution.

The formation constant for the Pb^{2+} -EDTA complex is high, at 1.1×10^{18} [35] (p. 315). In a basic buffer solution with pH 10, the formation constant remains high at 3.3×10^{17} . The complex formation is therefore expected to proceed to completion, according to Reaction (10):



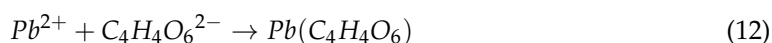
where H_2Y^{2-} is the EDTA acid and PbY^{2-} is the Pb^{2+} -EDTA complex.

The titration of Pb^{2+} with EDTA followed these steps:

- (1) An aliquot of the Pb^{2+} solution collected after centrifuging was diluted a 100 times. The solution was made to 25 cm^3 .
- (2) To make the solution basic, 5 mm of pH 10 ammonium hydroxide was added to the solution. This resulted in formation of solid $Pb(OH)_2$.



- (3) To keep the Pb^{2+} ions in solution, a spatula tip of powder tartaric acid was added. Tartaric acid complexes weakly with Pb^{2+} ions, keeping the Pb^{2+} ions aqueous.

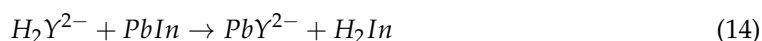


- (4) Before titration, a colour indicator was added to the solution. The indicator was prepared by grinding 100 mg of Erio Black T with 5 g of KCl. The indicator attaches to Pb^{2+} ions to form a reddish violet coloured complex, as indicated by Equation (13):



where In is the indicator.

- (5) A standard solution of $0.01 \text{ mol}\cdot\text{dm}^{-3}$ EDTA was titrated out of a burette into the solution under investigation.
- (6) The EDTA replaced the indicator from the $PbIn$ complex to form the strongly bonding PbY^{2-} until the indicator existed as a free protonated dye with a blue colour. Replacement of the indicator by EDTA is shown in Equation (14):



At the end-point, the colour of the solution changed from violet to blue.

- (7) The concentration of lead in the solution was related to the concentration of EDTA by the equation:

$$C_{EDTA} V_{EDTA} = [Pb^{2+}] V_{Pb^{2+}} \quad (15)$$

The concentration obtained from the titration experiments was recorded and compared to the concentration estimates made from density measurements.

2.6.4. Cyclic Voltammetry

A three-electrode electrochemical cell was used to determine the presence of Pb^{2+} ions in solution. A rotating disc electrode was used to control the mass transport properties of the system, and electrolyte flow was kept laminar. The cell used a vitreous carbon working electrode (WE) with an area of 0.1527 cm^2 , a saturated standard calomel electrode (SCE) and a 1.5 cm^2 platinum wire mesh counter electrode (CE), shown in Figure 4.

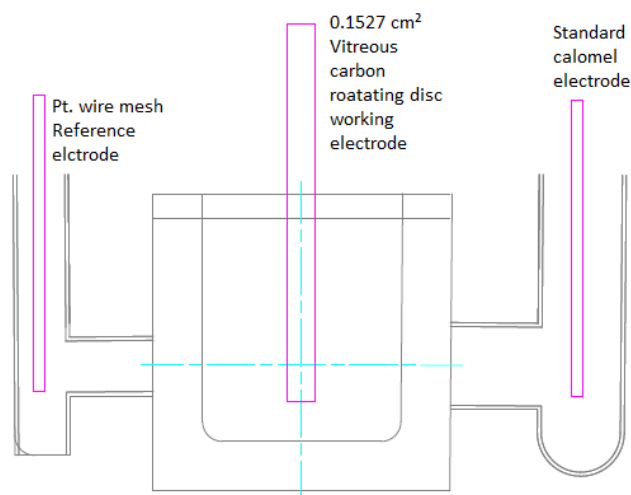


Figure 4. Sketch of three-electrode cell for cyclic voltammetry with 1.2 cm^2 Pt wire mesh reference electrode, 0.1527 cm^2 vitreous carbon rotating disc working electrode and a saturated calomel standard electrode.

Cyclic voltammetry experiments were carried out on diluted recovered electrolyte. The WE was polished on a Buehler 736-3 8" microcloth with $0.3 \mu\text{m}$ alumina suspended in water. The WE was rotated at 800 rpm, and a potential sweep was applied at $25 \text{ mV}\cdot\text{s}^{-1}$. The experiments were carried out at room temperature. For the Pb/Pb^{2+} couple voltammetry, the potential was swept between -0.8 V and -0.3 V . For the $\text{PbO}_2/\text{Pb}^{2+}$, the potential was swept between 0.2 V and 1.9 V . The electrolyte used was $1 \text{ mol}\cdot\text{dm}^{-3}$ MSA.

2.6.5. Flow Cell Testing

The recovered electrolyte was subjected to an initial comparison to an electrolyte manufactured from fresh laboratory reagents. Each electrolyte comprised $0.9 \text{ mol}\cdot\text{dm}^{-3}$ Pb^{2+} in $0.7 \text{ mol}\cdot\text{dm}^{-3}$ MSA. The flow cell has been described previously [17] and comprised a parallel plate reactor with electrode surface areas of 10 cm^2 . The electrolyte was maintained at room temperature and pumped through the cell at a rate of $0.44 \text{ dm}^3\cdot\text{s}^{-1}$ using a Watson Marlow 505S peristaltic pump.

3. Results and Discussion

3.1. State of Health of Lead Acid Battery

The VRLA battery manual states that at $25 \text{ }^\circ\text{C}$, a battery voltage of 12.6 V corresponds to 100% SoC while an open circuit voltage under 11.8 V indicates 0% SoC [30]. Upon testing, the maximum battery open circuit voltage measured was 11.6 V , well below the 0% SoC mark. Therefore, these batteries were considered to have reached the end of their lives.

The Ah charge capacity of the batteries was less than 1% of the nominal capacity. This was another indicator that the batteries had reached the end-of-life. Using this indicator, along with the open circuit voltage, the batteries were chosen for lead recovery.

3.2. Lead Recovered

3.2.1. Recovered Electrolyte Qualitative Analysis

The presence of metal ions in the recovered electrolyte sample was confirmed using ICP-MS. As expected for the VRLA battery used, the presence of Ca^{2+} ions was confirmed. Bi^{2+} , Sn^{2+} and Sb^{2+} ions were also detected and quantified. The average concentration of Pb^{2+} ions averaged was $0.95 \text{ mol}\cdot\text{dm}^{-3}$, while that of Ca^{2+} and Sn^{2+} ions was $2.98 \times 10^{-6} \text{ mol}\cdot\text{dm}^{-3}$ and $0.08 \times 10^{-6} \text{ mol}\cdot\text{dm}^{-3}$, respectively. Bi^{2+} and Sb^{2+} ions had the lowest average concentrations at 0.99×10^{-9} and $0.44 \times 10^{-9} \text{ mol}\cdot\text{dm}^{-3}$ each.

The concentration of Pb^{2+} ions in the recovered electrolyte is three orders of magnitude higher than that of Ca^{2+} ions. The rest of the ions were present in parts per billion. Based on these quantities, the presence of the last three ions was considered to be negligible. Electrochemically calcium ions were not expected to affect performance of the recovered electrolyte.

3.2.2. Cyclic Voltammetry

The cyclic voltammograms for both the negative and positive electrodes are shown in Figure 5 and they are comparable to that found in literature [16].

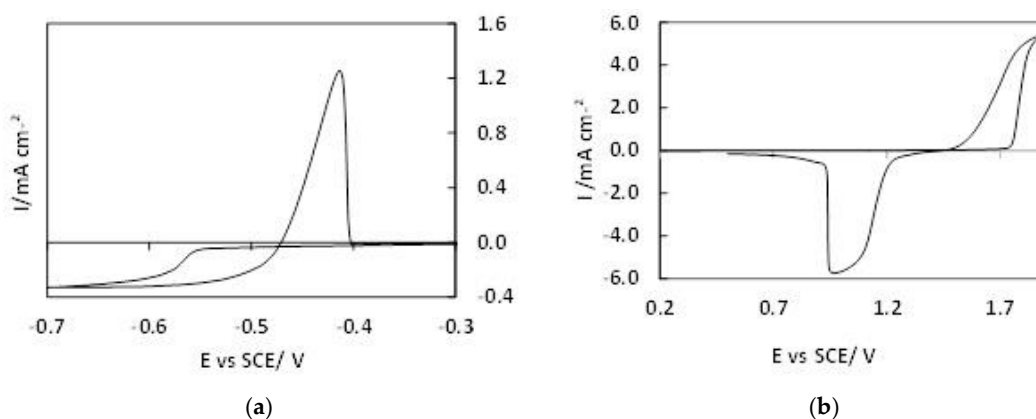


Figure 5. Cyclic voltammetry results of recovered electrolyte: $1 \text{ mol}\cdot\text{dm}^{-3}$ MSA using a vitreous carbon rotating disk working electrode (WE), rotated at 800 rpm, with a Pt wire reference electrode (RF) and standard calomel electrode (SCE), where a potential sweep was applied at $25 \text{ mV}\cdot\text{s}^{-1}$, at room temperature. (a) For the Pb/Pb^{2+} couple, the potential was swept between -0.7 V and -0.2 V . (b) For the $\text{PbO}_2/\text{Pb}^{2+}$, the potential was swept between 0.2 V and 1.9 V .

The characteristic deposit and anodic stripping of lead on the negative electrode (Figure 5a) is similar to that published by others, as is the behaviour at the positive electrode which is shown in Figure 5b [16].

3.2.3. Comparison of Methods Used to Quantify Lead (II) Ions Recovered

The quantity of Pb^{2+} ions recovered was monitored by checking solution density, as well as by titration. Table 3 compares sample values of Pb^{2+} ions concentration calculated using the change in mass of the solution as well as titration. Calculations of $[\text{Pb}^{2+}]$ concentrations using mass of the solution recovered and using titration were performed using Equation (9) for the mass measurements and Equation (15) for titration.

Table 3. Comparison of the concentration of Pb^{2+} ions obtained by mass measurements and by titration. The variance between the two values is lower than 10% in all cases.

[Pb^{2+}] in $\text{mol}\cdot\text{dm}^{-3}$ by		%Variance
Mass Measurements	Titration	
0.65	0.656	0.9
0.68	0.670	1.5
0.73	0.716	1.9
0.87	0.860	1.2
0.95	0.890	6.3
0.96	0.900	6.3
1.06	0.930	9.7

The concentration of Pb^{2+} ions calculated from the change in mass of the solution differs from that obtained by titration measurements by less than 10%. The mass measurements could therefore be considered a reliable method. The close agreement of the results also confirms that the assumption that the change in mass of the solution was due to Pb and PbO_2 solids being converted to Pb^{2+} ions was reasonable.

It is worth noting that the difference between the values from the two methods lessened the longer the sample was allowed to settle. In those cases, it was not necessary to centrifuge the sample before aliquots were collected.

There were concerns about interference from calcium (II) ions complexing with EDTA, since calcium (II) ions complex with EDTA at the same pH as do lead (II) ions. However, because of the much higher formation constant of Pb-EDTA (1.1×10^{18}) as compared to Ca-EDTA (5.0×10^{10}), the Pb-EDTA complex is expected to reach equivalence before the Ca-EDTA complex is formed, hence the titration results are considered reliable.

3.2.4. Quantity of Lead (II) Ions Recovered

The methods described in Section 2.5 and by Figure 3 yielded different concentrations of lead Pb^{2+} ions. Table 4 shows the results for each method.

Table 4. Amount of Pb^{2+} ions in the solution made by dissolving solid VRLA battery electrodes. The temperatures shown are averaged over 6 h.

Method	Electrode Material (g)	Average Temperature ($^{\circ}\text{C}$)	[H_2O_2] ($\text{mol}\cdot\text{dm}^{-3}$)	[Pb^{2+}] ($\text{mol}\cdot\text{dm}^{-3}$)
1	250	30	-	0.16
2	250	45	-	0.07
3	250	30	0.09	0.51
4	250	40	0.09	0.75
5	250	30	0.90	1.00
6	250	40	0.90	0.91

The density of the collected samples tended to stabilise after six hours and it was found that without hydrogen peroxide, the amount of lead (II) ions recovered was lower than 0.2 M. Addition of $0.09 \text{ mol}\cdot\text{dm}^{-3}$ H_2O_2 yielded 0.5 M, which was half the required amount of Pb^{2+} . Solutions with the highest concentration of H_2O_2 yielded the highest concentration of Pb^{2+} ions, and the required $1.0 \text{ mol}\cdot\text{dm}^{-3}$ was obtained.

The quantity of hydrogen peroxide was kept at 10% of the total volume to control reaction volatility. The concentration of recovered electrolyte was limited at $1.0 \text{ mol}\cdot\text{dm}^{-3}$ of Pb^{2+} ions by the initial concentration of acid. It was possible to recover more Pb^{2+} ions by adding more acid and hydrogen peroxide.

3.3. Flow Cell

Comparison of Recovered and Standard Electrolytes

An initial comparison of the recovered electrolyte to a standard electrolyte, manufactured using fresh laboratory reagents, was carried out in a small (10 cm² electrode area) flow cell. The voltage profile was similar for both electrolytes and consistent with previously reported data [16]. Each electrolyte was subjected to 20 cycles in the flow cell, where each cycle consisted of a 1 h period of charge at 20 mA·cm⁻² followed by full discharge at 20 mA·cm⁻². The average charge, energy and voltage efficiency obtained for each electrolyte is shown in Table 5. There was no difference in the voltage efficiency, although the recovered electrolyte returned charge and energy efficiencies 4% and 2% respectively lower than the standard electrolyte. This is a relatively small variation and within deviations typically observed in the literature [17]. The similarity in performance between the recovered and standard electrolytes is encouraging and further characterisation of the recovered electrolyte within an operational flow cell is ongoing.

Table 5. Operational data from 10 cm² flow cell, comparing electrolyte recovered from conventional lead acid batteries using the methodology detailed in this paper and standard electrolyte manufactured from laboratory reagents.

Electrolyte	Charge Efficiency/%	Energy Efficiency/%	Voltage Efficiency/%
Recovered	81	52	64
Standard	85	54	64

4. Conclusions

A novel lead recovery method for making electrolyte for a soluble lead redox flow battery has been developed by the authors using methanesulfonic acid and hydrogen peroxide. The method involved dissolving spent lead acid electrodes in warm MSA and using hydrogen peroxide to catalyse the oxidation and reduction of solid Pb (IV) and Pb, respectively.

The method successfully yielded the amount of lead (II) ions (0.9 to 1.5 mol·dm⁻³) sought, over a period of at least 6 h. The methods used to recover lead yielded varying amounts of lead (II) ions, indicating that some were more favourable than others. The addition of hydrogen peroxide catalysed the retrieval of lead ions from lead (IV) oxide. As shown by the cyclic voltammetry results, the recovered electrolyte displays similar electrochemical activity as does the conventional electrolyte used in soluble lead redox flow batteries developed by others. A lead (II) concentration of 1.5 mol·dm⁻³ would give an equivalent storage capacity of 40 Ahr·dm⁻³ of electrolyte or 60 Whr·dm⁻³ (at a discharge voltage of 1.5 V).

A comparison of recovered and standard (made from laboratory reagents) electrolytes in an operational flow cell showed encouraging performance. Further, detailed characterisation of the recovered electrolyte in a flow cell environment is planned to enable optimisation of the recovery process and electrolyte composition. The ability to reprocess waste conventional lead acid batteries at the end of their useful life offers a novel and low cost route to obtaining an electrolyte for the soluble lead flow battery. Further work should be carried out to compare the energy requirements for this process and traditional lead acid recycling. A low cost, abundant supply of electrolyte for the soluble lead flow battery would have a significant impact on future commercialisation of the technology.

Acknowledgments: This research was carried out with the financial support of the Government of Botswana as well as the Botswana International University of Science and Technology.

Author Contributions: Richard G. A. Wills and Andrew Cruden conceived and designed the experiments, Keletso Orapeleng performed the experiments and analyzed the data, Richard G. A. Wills contributed reagents and materials, Andrew Cruden contributed laboratory equipment and Keletso Orapeleng wrote the paper. Andrew Cruden and Richard G. A. Wills proof-read.

Conflicts of Interest: The authors declare no conflict of interest.

References

1. Teller, O.; Nicolai, J.-P.; Lafoz, M.; Laing, D.; Tamme, R.; Pedersen, A.S.; Andersson, M.; Folke, C.; Bourdil, C.; Conte, M.; et al. *Joint EASE/EERA Recommendations for a European Energy Storage Technology Development Roadmap Towards 2030*; Martens, D., Ed.; European Association for Storage of Energy (EASE) and European Energy Research Alliance (EERA): Brussels, Belgium, 2013; pp. 1–226.
2. Spiers, D.J.; Rasinkoski, A.D. Predicting the service lifetime of lead/acid batteries in photovoltaic systems. *J. Power Sources* **1995**, *53*, 245–253. [[CrossRef](#)]
3. Jossen, A.; Garche, J.; Sauer, D.U. Operation conditions of batteries in PV applications. *Sol. Energy* **2004**, *76*, 759–769. [[CrossRef](#)]
4. Garche, J.; Jossen, A.; Döring, H. The influence of different operating conditions, especially over-discharge, on the lifetime and performance of lead/acid batteries for photovoltaic systems. *J. Power Sources* **1997**, *67*, 201–212. [[CrossRef](#)]
5. Salkind, A.J.; Cannone, A.G.; Trumbure, F.A. Lead-acid batteries. In *Handbook of Batteries*; Linden, D., Reddy, T., Eds.; McGraw-Hill: New York, NY, USA, 2002.
6. Ponce de León, C.; Frías-Ferrer, A.; González-García, J.; Szánto, D.A.; Walsh, F.C. Redox flow cells for energy conversion. *J. Power Sources* **2006**, *160*, 716–732. [[CrossRef](#)]
7. Alotto, P.; Guarnieri, M.; Moro, F. Redox flow batteries for the storage of renewable energy: A review. *Renew. Sustain. Energy Rev.* **2014**, *29*, 325–335. [[CrossRef](#)]
8. Weber, A.; Mench, M.; Meyers, J.; Ross, P.; Gostick, J.; Liu, Q. Redox flow batteries: A review. *J. Appl. Electrochem.* **2011**, *41*, 1137–1164. [[CrossRef](#)]
9. Akhil, A.A.; Huff, G.; Currier, A.B.; Kaun, B.C.; Rastler, D.M.; Chen, M.C.; Cotter, A.L.; Bradshaw, D.T.; Gauntlett, W.D. *DOE/EPRI 2013 Electricity Storage Handbook in Collaboration with NRECA*; Sandia National Laboratories: Albuquerque, NM, USA; Livermore, CA, USA, 2013.
10. Pletcher, D.; Wills, R. A novel flow battery: A lead acid battery based on an electrolyte with soluble lead(II) Part II. Flow cell studies. *Phys. Chem. Chem. Phys.* **2004**, *6*, 1779–1785. [[CrossRef](#)]
11. Cunha, Á.; Martins, J.; Rodrigues, N.; Brito, F.P. Vanadium redox flow batteries: A technology review. *Int. J. Energy Res.* **2015**, *39*, 889–918. [[CrossRef](#)]
12. Verde, M.G.; Carroll, K.J.; Wang, Z.; Sathrum, A.; Meng, Y.S. Achieving high efficiency and cyclability in inexpensive soluble lead flow batteries. *Energy Environ. Sci.* **2013**, *6*, 1573–1581. [[CrossRef](#)]
13. Skyllas-Kazacos, M.; Kazacos, G.; Poon, G.; Verseema, H. Recent advances with UNSW vanadium-based redox flow batteries. *Int. J. Energy Res.* **2010**, *34*, 182–189. [[CrossRef](#)]
14. Perrin, M.; Saint-Drenan, Y.M.; Mattera, F.; Malbranche, P. Lead-acid batteries in stationary applications: Competitors and new markets for large penetration of renewable energies. *J. Power Sources* **2005**, *144*, 402–410. [[CrossRef](#)]
15. Skyllas-Kazacos, M.; Chakrabarti, M.H.; Hajimolana, S.A.; Mjalli, F.S.; Saleem, M. Progress in flow battery research and development. *J. Electrochem. Soc.* **2011**, *158*, R55–R79. [[CrossRef](#)]
16. Hazza, A.; Pletcher, D.; Wills, R. A novel flow battery: A lead acid battery based on an electrolyte with soluble lead(II) Part I. Preliminary studies. *Phys. Chem. Chem. Phys.* **2004**, *6*, 1773–1778. [[CrossRef](#)]
17. Collins, J.; Kear, G.; Li, X.; Low, C.T.J.; Pletcher, D.; Tangirala, R.; Stratton-Campbell, D.; Walsh, F.C.; Zhang, C. A novel flow battery: A lead acid battery based on an electrolyte with soluble lead(II) Part VIII. The cycling of a 10 cm × 10 cm flow cell. *J. Power Sources* **2010**, *195*, 1731–1738. [[CrossRef](#)]
18. Collins, J.; Li, X.; Pletcher, D.; Tangirala, R.; Stratton-Campbell, D.; Walsh, F.C.; Zhang, C. A novel flow battery: A lead acid battery based on an electrolyte with soluble lead(II). Part IX: Electrode and electrolyte conditioning with hydrogen peroxide. *J. Power Sources* **2010**, *195*, 2975–2978. [[CrossRef](#)]
19. Wills, G.A.R. *A Lead Acid Flow Battery for Utility Scale Energy Storage and Load Levelling*; Soton eprints; Faculty of Chemistry, University of Southampton: Southampton, UK, 2004; p. 153.
20. Pletcher, D.; Zhou, H.; Kear, G.; Low, C.T.J.; Walsh, F.C.; Wills, R.G.A. A novel flow battery—A lead-acid battery based on an electrolyte with soluble lead(II) V. Studies of the lead negative electrode. *J. Power Sources* **2008**, *180*, 621–629. [[CrossRef](#)]

21. Battery Council International. *National Recycling Rate Study*; SmithBucklin Statistics Group: Chicago, IL, USA, 2014.
22. Ellis, T.W.; Mirza, A.H. The refining of secondary lead for use in advanced lead-acid batteries. *J. Power Sources* **2010**, *195*, 4525–4529. [CrossRef]
23. Yuasa Battery Inc. *NP Series: NP7-12*; Yuasa Battery Inc.: Laureldale, PA, USA, 2008.
24. MacFarlane, D.R.; Pringle, J.M.; Howlett, P.C.; Forsyth, M. Ionic liquids and reactions at the electrochemical interface. *Phys. Chem. Chem. Phys.* **2010**, *12*, 1659–1669. [CrossRef] [PubMed]
25. Gernon, M.; Wu, M.; Buszta, T.; Janney, P. Environmental benefits of methanesulfonic acid. Comparative properties and advantages. *Green Chem.* **1999**, *1*, 127–140. [CrossRef]
26. Pletcher, D.; Zhou, H.; Kear, G.; Low, C.T.J.; Walsh, F.C.; Wills, R.G.A. A novel flow battery—A lead-acid battery based on an electrolyte with soluble lead(II) Part VI. Studies of the lead dioxide positive electrode. *J. Power Sources* **2008**, *180*, 630–634. [CrossRef]
27. Ropp, R.C. Chapter 5—Group 14 (C, Si, Ge, Sn, and Pb) alkaline earth compounds. In *Encyclopedia of the Alkaline Earth Compounds*; Elsevier: Amsterdam, The Netherlands, 2013; pp. 351–480.
28. Pavlov, D. Chapter 14—Methods to restore the water decomposed during charge and overcharge of lead-acid batteries. VRLA Batteries. In *Lead-Acid Batteries: Science and Technology*; Elsevier: Amsterdam, The Netherlands, 2011; pp. 567–603.
29. IEEE-SA. IEEE recommended practice for maintenance, testing, and replacement of valve-regulated lead-acid (VRLA) batteries for stationary applications. In *IEEE Std 1188-2005 (Revision of IEEE Std 1188-1996)*; American National Standards Institute: New York, NY, USA, 2006; pp. 1–44.
30. Yuasa Technical Manual. Available online: <http://ktm950.info/library/assets/pdfs/Yuasa%20Batteries.pdf> (accessed on 4 December 2015).
31. Finger, P.E.; Boden, D. Electrode materials. In *Battery Book 2*; Curtis Instruments Inc.: Mt Kisco, NY, USA, 2007.
32. Moseley, P.T.; Rand, D.A.J. Chapter 1—The valve-regulated battery—A paradigm shift in lead-acid technology. In *Valve-Regulated Lead-Acid Batteries*; Rand, D.A.J., Garche, J., Moseley, P.T., Parker, C.D., Eds.; Elsevier: Amsterdam, The Netherlands, 2004; pp. 1–14.
33. Prengaman, R.D.; Rand, D.A.J. Chapter 2—Lead alloys for valve-regulated lead-acid batteries A2. In *Valve-Regulated Lead-Acid Batteries*; Rand, D.A.J., Garche, J., Moseley, P.T., Parker, C.D., Eds.; Elsevier: Amsterdam, The Netherlands, 2004; pp. 15–35.
34. Fitch, A. Lead analysis: Past and present. *Crit. Rev. Anal. Chem.* **1998**, *28*, 267–345. [CrossRef]
35. Vogel, A.I.; Jeffery, G.H. *Vogel's Textbook of Quantitative Chemical Analysis*; Longman Scientific & Technical: London, UK, 1989.



© 2017 by the authors. Licensee MDPI, Basel, Switzerland. This article is an open access article distributed under the terms and conditions of the Creative Commons Attribution (CC BY) license (<http://creativecommons.org/licenses/by/4.0/>).